INFLUENȚA DURATEI DE TRATAMENT TERMIC ASUPRA PROCESULUI DE SINTEZĂ A GYROLITULUI
THE INFLUENCE OF HYDROTHERMAL TREATMENT DURATION ON GYROLITE SYNTHESIS

ALIONA ILJINA* , KESTUTIS BALTAKYS, ANATOLIJUS EISINAS

[1] *Department of Silicate Technology, Kaunas University of Technology, Radvilenu 19, LT–50270 Kaunas, Lithuania*

The influence of hydrothermal synthesis duration at 200°C temperature on the crystallinity and stability of gyrolite was determined. Gyrolite was synthesized for 120, 168, 336, and 504 h at 200°C from a stoichiometric composition (molar ratio of CaO/SiO_2 = 0.66) of the initial CaO and SiO_2nH_2O mixture. It was determined that after 120 – 168 h of hydrothermal synthesis, gyrolite formed as the final product, because the increment of the intensities (from 112.55 to 130.57 a. u.) and crystallite size (from 46.2 nm to 55.3 nm) of the main diffraction peak (d ~ 2.273 nm) were observed. Meanwhile, after 336 – 504 h of treatment, gyrolite became metastable because traces of a new compound of calcium silicate hydrate – truscottite were formed. The calculated thermodynamic parameters of hypothetical recrystallization reactions of gyrolite confirmed the obtained experimental results: the formation of truscottite is more possible because the obtained Gibbs free energy value of this compound is the lowest one (ΔG = -39.8 kJ). Also, it was determined that the duration of hydrothermal synthesis has influence on the gyrolite specific surface area, dominant pore size and their differential distribution by the radius. It should be noted that synthetic gyrolite can be used as adsorbent for Zn^{2+} ions removal, because its adsorption capacity (27.91 mg Zn^{2+}/g) is higher than natural clinoptilolite (25.00 mg Zn^{2+}/g).

Keywords: *gyrolite, truscottite, calcium-silicate-hydrate, hydrothermal synthesis, specific surface area*

1. Introduction

Among the numerous calcium silicate hydrates (C-S-H) occurring in the ternary system $CaO-SiO_2-H_2O$, the interest in gyrolite has grown considerably in recent years [1]. This arises from the fact that gyrolite similarly to some other calcium silicate hydrates – tobermorite, xonotlite or C-S-H(I) has cation exchange capacity [2–6]. It was determined that gyrolite can adsorb more chemical elements than other C-S-H because the interlayer sheets with a thickness of about 2.2 nm in gyrolite are available for the intercalation of a new guest by controlling the charge of the host [7]. For this reason this compound is very good immobilizer for toxic ions, heavy metals, and organic compounds [8-12]. Therefore, it is important to ascertain the structural changes of gyrolite under conditions of hydrothermal synthesis. Hydrothermal synthesis of gyrolite is a long and complex process. However, this compound is usually prepared from an aqueous suspension of CaO and various forms of SiO_2 by hydrothermal treatment at temperatures of about 200°C, where the molar ratio of CaO/SiO_2 equals to 0.66. E. P. Flint et al., who first synthesized gyrolite, reported that after 6–42 days of hydrothermal treatment at 150–350°C temperature, when the molar ratio of the starting materials changes from 0.5 to 0.66 the only product of synthesis was gyrolite [13]. Meanwhile, Mackay and Taylor [14] synthesized this compound at 150°C temperature within 76 days of isothermal curing.

Moreover, Kalousek and Nelson [15], and also Stevula and Petrovic [16] found that gyrolite could likewise be prepared by interacting of dicalcium silicate ($2CaO·SiO_2$) with SiO_2 in aqueous suspension under hydrothermal conditions. Kalousek and Nelson have determined that under hydrothermal conditions, gyrolite is stable at 200°C temperature, meanwhile at 300°C temperature truscottite was formed [15].

Later on, other scientists continued the studies on the synthesis of gyrolite [17–19]. It was declared that gyrolite is stable at 120–200°C temperature in hydrothermal conditions under the saturated steam pressure. Truscottite forms at a temperature higher than 200°C, although a metastable gyrolite may be obtained up to 270°C. It is assumed that gyrolite forms only at a temperature higher than 120°C. At a lower temperature, a semicrystalline phase having no crystal structure (C-S-H gel) is obtained. At variable C/S ratio, the formation of other calcium silicate hydrates, which are stable at the given conditions (pressure, temperature), takes place. Therefore, C-S-H gel is transformed into a semicrystalline C-S-H (I). However, at sufficiently long hydrothermal treatment, this compound may turn into metastable

* Autor corespondent/*Corresponding author,*
E-mail: aliona.iljina@gmail.com

phase, due to the formation of gyrolite. It has been shown that while synthesizing gyrolite, an intermediary compound Z-phase [20] often forms, with a 1.5 nm basic reflection characteristic.

Shaw et al. [19] had utilized a synchrotron source of high-energy X-rays and energy-dispersive powder diffraction and presented the information about compound formation sequence in the hydrothermal crystallization of gyrolite at a temperature range of 190–240°C. They found that Z-phase probably has no stability field, which supports the idea that Z-phase is a transient, metastable phase in the formation of gyrolite.

Also, conditions for the formation and stability of gyrolite have been extensively studied by Baltakys and Siauciunas [21]. It was determined the influence of SiO_2 modification on crystallization process of gyrolite. Authors showed that gyrolite does not form even during a week in the mixtures of CaO and amorphous SiO_2 at 150°C under the saturated steam pressure. The temperature increase positively affects synthesis of this compound – pure gyrolite is produced at 175°C after 72 h, and after 32 h – at 200°C. It should be underlined that in the mixtures with quartz the mechanism of compound formation is quite different. Due to a low quartz solubility rate at temperature range from 150 to 200°C, neither Z-phase, nor gyrolite is formed even after 72 h of hydrothermal curing. α-C_2S hydrate and C-S-H(II) prevail in the beginning of the synthesis and gradually recrystallizes into 1.13 nm tobermorite and xonotlite. However, there is only a little data in the literature on structural changes of gyrolite under conditions of hydrothermal synthesis when the synthesis duration is higher than one week [11].

The aim of this work was to determine the influence of hydrothermal synthesis duration at 200°C temperature on the crystallinity and stability of gyrolite.

2. Materials and methods

2.1. Materials and manufacture of synthetic gyrolite

In this work the following reagents were used as starting materials: calcium oxide, which has been produced by burning calcium hydroxide (Stanchem, Poland) at 950°C for 30 minutes and ground to reach the specific surface area S_a of 1171 $m^2\ kg^{-1}$ by a CILAS LD 1090 granulometer, with the quantity of free CaO equal to 97.68%; fine ground $SiO_2 \cdot nH_2O$ (Reaktiv, Russia), having a specific surface area S_a = 1307 $m^2\ kg^{-1}$, with loss of ignition – 21.28%; natural zeolite – clinoptilolite of Carpathians quarry (Ukraine); S_a = 793 $m^2\ kg^{-1}$.

The synthesis of gyrolite was carried out in unstirred suspensions in vessels of stainless steel. Pure gyrolite was synthesized for 120, 168, 336, and 504 h at 200°C from a stoichiometric composition (the molar ratio of CaO/SiO_2 was equal to 0.66 and the water/solid ratio of the suspension was equal to 10.0) of the initial CaO and SiO_2nH_2O mixture. These synthesis conditions were chosen according to previously published data [21]. The products of the synthesis were filtered, rinsed with ethyl alcohol to prevent carbonation of materials, dried at 50 ± 5°C, and sieved through a sieve with a mesh width of 50 μm.

2.2 Analytical techniques

The XRD analysis were performed on the D8 Advance diffractometer (Bruker AXS, Karlsruhe, Germany) operating at the tube voltage of 40 kV and tube current of 40 mA. The X-ray beam was filtered with Ni 0.02 mm filter to select the CuKα wavelength. Diffraction patterns were recorded in a Bragg-Brentano geometry using a fast counting detector Bruker LynxEye based on silicon strip technology. The step-scan covered the angular range 3–70° (2θ) in steps of 2θ = 0.02° at a scanning speed of $6°\cdot min^{-1}$ using a coupled two theta/theta scan type. A XRD software "Diffrac.Eva" was used for the calculation of crystallite size and intensities of synthesis products. Scherrer's equation was used for the calculation of crystallite size (D_{hkl}):

$$D_{hkl} = \frac{k \cdot \lambda}{B_{hkl} \cdot \cos\theta} \qquad \text{(Eq. 1)}$$

where λ is the wavelength of the Cu Kα radiation, θ is Bragg's diffraction angle, B_{hkl} is the full width at half maximum intensity, and k is a constant (the value used in this study was 0.94).

Simultaneous thermal analysis (STA), differential scanning calorimetry (DSC) and thermogravimetry (TG)) was also employed to measure the thermal stability and phase transformation of samples at a heating rate of 15°C/min; the temperature ranged from 30°C up to 1000°C under air atmosphere. The test was carried out on a Netzsch instrument STA 409 PC Luxx. Ceramic sample handlers and crucibles of Pt-Rh were also used.

Infrared spectra were carried out with the help of a Perkin Elmer FT-IR Spectrum X system. Specimens were prepared by mixing 1 mg of the synthesized product with 200 mg of KBr. The spectral analysis was performed in the range of 4000–400 cm^{-1} with spectral resolution of 1 cm^{-1}.

For the thermodynamic calculations of the hypothetical reaction parameters, the values of enthalpy $\left(\Delta H^{o,f}_{298}\right)$, entropy $\left(S^{o,f}_{298}\right)$ and molar specific heat capacities (C_p) of the formed compounds are applied and given in Table 1. For the estimations we used a method of absolute entropies, according to which the change of

reaction standard free Gibbs energy $\Delta_r G_T^0$ can be calculated by the equation:

$$\Delta_r G_T^0 = \Delta_r H_T^0 - T\Delta_r S_T^0, \quad \text{(Eq. 2)}$$

where $\Delta_r H_T^0$ and $\Delta_r S_T^0$ are the change/alteration/variation of reaction enthalpy and entropy in temperature T. Enthalpy and entropy for the reaction can be calculated form the equations:

$$\Delta_r H_T^0 = \Delta_r H_{298}^0 + \Delta C_p(T_1 - 298), \quad \text{(Eq. 3)}$$

$$\Delta_r S_T^0 = \Delta_r S_{298}^0 + \Delta C_p\left(\frac{T_1}{298}\right), \quad \text{(Eq. 4)}$$

where $\Delta_r H_{298}^0$ is the standard enthalpy change of the reactions, J/mol; $\Delta_r S_{298}^0$ is the standard entropy change of the reactions, J/mol; and $\Delta_r a$, $\Delta_r b$, $\Delta_r c$, and $\Delta_r c'$ are the constants of heat capacity dependence on temperature. The standard molar thermodynamic properties values at 25 ºC and 1 bar (Table 1) were taken from the literature [22, 23].

The surface area, total pore volume and pore size distribution of the synthesis products were performed by a BET surface area analyzer ''KELVIN 1042 Sorptometer'' (Costech Instruments).

The specific surface area of gyrolite was calculated by the BET equation using the data of the lower part of N_2 adsorption isotherm ($0.05 < p/p_0 < 0.35$):

$$\frac{1}{X\left(\frac{p_0}{p} - 1\right)} = \frac{C-1}{X_m \cdot C} \cdot \frac{p}{p_0} + \frac{1}{X_m \cdot C}, \quad \text{(Eq. 5)}$$

where X is the mass of adsorbate, adsorbed on the sample at relative pressure p/p_0, p the partial pressure of adsorbate, p_0 the saturated vapour pressure of adsorbate, X_m the mass of adsorbate adsorbed at a coverage of one monolayer, C is a constant which is a function of the heat of the adsorbate condensation and heat of adsorption (C_{BET} is a constant).

BET equation yields a straight line when $1/X[(p_0/p) - 1]$ is plotted versus p/p_0. The slope of $(C - 1)/X_mC$ and the intercept of $1/X_mC$ was used to determine X_m and C: S = slope = $(C - 1)/X_mC$ and I = intercept = $1/X_mC$. Solving for X_m yields $X_m = 1/(S + I)$. BET plot is usually found to be linear in the range $p/p_0 = 0.05–0.35$. The total surface area of the sample S_t was determined by the equation $S_t = X_m N A_{cs}/M$, where M is the molecular mass of the adsorbate, N the Avogadro's constant, A_{cs} the cross-sectional area occupied by each nitrogen molecule (16.2×10^{-20} m^2). The specific surface area was given by the equation $S_{BET} = S_t/m$, where m is the mass of synthesis product sample.

The total pore volume and pore size distribution were calculated according to the corrected Kelvin equation and Orr et al. scheme [27, 28] using entire N_2 desorption isotherm at 77 K. The Kelvin equation relates the adsorbate vapour pressure depression to the radius of a capillary which has been filled with adsorbate:

$$ln\frac{p}{p_0} = -2\frac{\gamma V_m \cos\theta}{R\,T\,r_k}, \quad \text{(Eq. 6)}$$

where p is the saturated vapour pressure in equilibrium with the adsorbate condensed in a capillary or pore, p_0 the normal adsorbate saturated vapour pressure, γ the surface tension of nitrogen at its boiling point ($\gamma = 8.85$ ergs/cm^2 at (-195.8°C)), V_m the molar volume of liquid nitrogen ($V_m = 34.7$ cm^3), θ the wetting angle (usually taken 0° and $\cos\theta = 1$), R the gas constant ($R = 8.134 \cdot 10^7$ ergs deg^{-1} mol^{-1}), T the absolute temperature ($T = 77$ K) and r_K the Kelvin radius of pore.

Table 1

Standard molar thermodynamic properties at 25 ºC and 1 bar

Material	$\Delta H_{298}^{o,f}$, kJ·mol^{-1}	$\Delta G_{298}^{0,f}$, kJ·mol^{-1}	ΔC_p, J·mol^{-1}·K^{-1}	$S_{298}^{o,f}$, J·mol^{-1}·K^{-1}
$H_2O_{(v)}$	-241.8	-228.6	33.2	188.7
SiO_2	-910.9	-856.6	44.5	41.8
$Ca(OH)_2$	-985.1	-897.5	87.4	83.3
Z-phase	-3135.8	-	161.9	170.9
gyrolite	-4914.4	-4550.1	325.9	271.2
1.4 nm tobermorite	-12175.1	-11090.1	973.5	874.5
1.1 nm tobermorite	-10680.9	-9889.2	764.9	692.5
Xonotlite	-10022.1	-9465.1	548.3	507.5
Okenite	-3135.7	-2881.7	210.0	208.5
Truscottite	-16854.6	-15280.4	1034.1	927.6

Adsorption experiments were carried out at 25 °C in the thermostatic absorber Grant SUB14 with different time periods (0.5, 1, 3, 5, 10, 25, 60 and 120 min). A series of suspensions in conical flasks were prepared, each containing 1 g of gyrolite (synthesized after 168 h) or clinoptilolite and 100 ml of 0.3 g×Zn^{2+}/dm^3 aqueous solutions. The percentage of adsorbed ions was determined using the variations of cations concentration both in the solution and in gyrolite or clinoptilolite. The concentration of Zn^{2+} ions in aqueous solution was determined using a Perkin Elmer AAnalyst 400 Atomic Absorption Spectrometer. All tests were repeated three times.

3. Results and discussions

It was determined that, in the CaO and $SiO_2 \cdot nH_2O$ mixture after 120 h of hydrothermal treatment when the molar ratio of the initial mixture CaO/SiO_2 ~ 0.66, gyrolite (*d*-spacing: 2.273, 1.126, 0.844, 0.420, 0.365, 0.280, and 0.224 nm) formed as the final product of synthesis (Fig. 1, curve 1). By extending the treatment duration to 168 h, the intensity of the main diffraction peak (*d* ~ 2.273) and the crystallite size of mentioned compound increased from 112.6 to 130.6 a. u (Table 2) as well as from 46.2 nm to 55.3 nm, respectively (Fig. 2, b).

Meanwhile, after extending the duration of isothermal curing to 336 h, gyrolite became metastable because traces of a new compound of calcium silicate hydrate – truscottite (*d*-spacing: 1.880, 0.942, 0.769, 0.471, 0.314, 0.183, and 0.176 nm) were formed (Figure 1, curve 3). The visible changes in the main diffraction peak (*d* ~ 2.273) of gyrolite can be seen in the Figure 2, a, because doublet peak with *d*-spacing 2.2047 nm and *d*-spacing 2.030 nm formed in 3 – 5° diffraction angles range (Figure 2, a, curves 2, 3).

On the other hand, the intensity of gyrolite diffraction peak significantly decreased (to 94.55 a. u.). Meanwhile, the peaks intensities of truscottite remained the same (~ 62 a. u) till 504 h (Table 2). At the same time, the crystallite size of gyrolite decreased from 56.1 nm to 52.3 nm, whereas the crystallite size of truscottite increased from 45.5 to 50.2 nm (Figure 2, b).

The presented results are only in a partial agreement with the data of Flint et al., which indicated that after 6–42 days of hydrothermal treatment at 150–350°C temperature, the only product – gyrolite – forms when C/S changes from 0.5 to 0.66 [13]. Meanwhile, Mackay and Taylor [14] have synthesized this compound at 150°C within 76 days of isothermal treatment. Later on, K. Garbev has synthesized gyrolite from C-S-H gel with C/S=0.66 after 10 days at 200°C and after 33 days at 220°C [24].

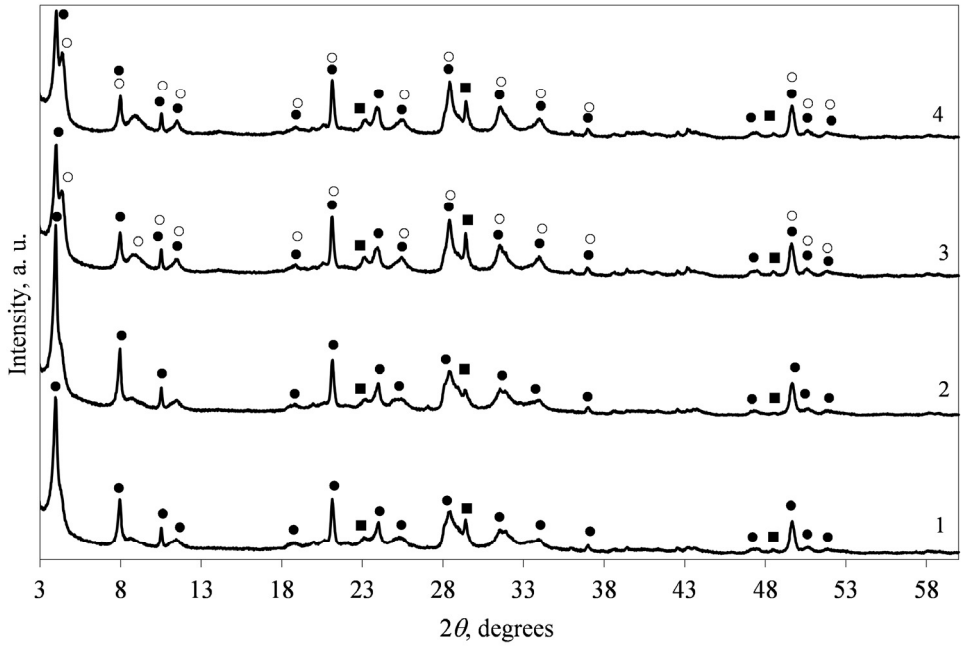

Fig. 1- X-ray diffraction patterns of synthesis product for varying durations of hydrothermal treatment at 200 °C, in h: 1 – 120, 2 – 168, 3 – 336, 4 – 504. Indexes: ● – gyrolite, ○ – truscottite, ■ – calcite.

Table 2

The intensities of the main gyrolite *d*-spacing (2.273 nm) and truscottite *d*-spacing (2.040 nm) diffraction Peaks

Duration of synthesis, h	Peak intensity of gyrolite ·10^2, a. u.	Peak intensity of truscottite ·10^2, a. u.
120	112.6	-
168	130.6	-
336	94.6	62.5
504	91.5	62.9

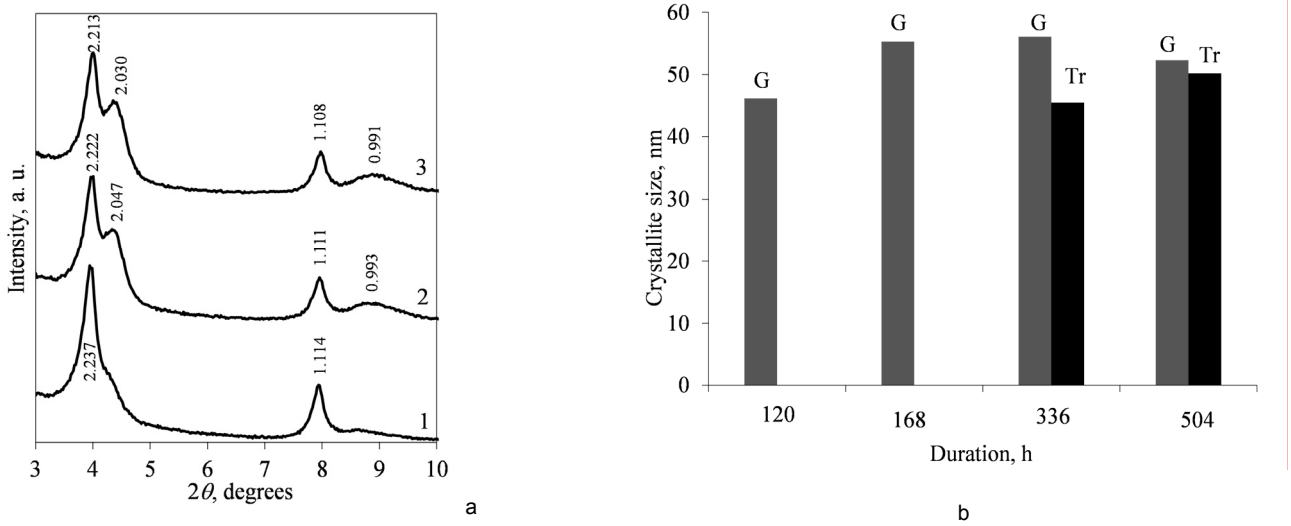

Fig. 2 - X-ray diffraction patterns (a) and crystallite size (b) of synthesis product with varying durations of hydrothermal treatment at 200°C, h: 1 – 120, 2 – 336, 3 – 504. Indexes: G – gyrolite, Tr – truscottite.

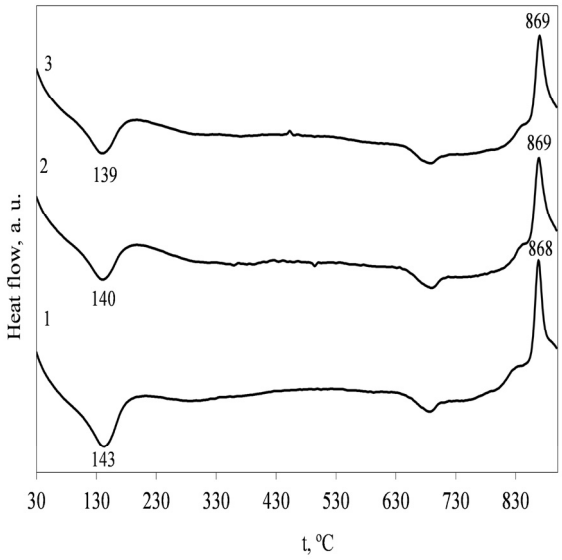

Fig. 3 - DSC curves of synthesis products with varying durations of hydrothermal treatment at 200 ° C, in h: 1 – 120, 2 – 336, 3 – 504.

The obtained results were confirmed by STA analysis data (Figure 3, Tables 3 and 4). On the DSC curve at 143–139°C temperature range, the broad endothermic peak is related to the loss of physisorbed and interlayer water from the crystal structure of synthesis products. This peak slightly decreased by prolonging synthesis duration to 504h (Figure 3, curve 3). The second exothermic peak (~870°C) is associated with recrystallization of this compound into wollastonite. Moreover, at ~700°C due to the decarbonation of synthesis products, a fair amount of formed calcium carbonate is also observed (Figure 3, curve 1-3).

It was observed that after 120–504 h of hydrothermal treatment, the heat of endothermic effects at 80–200C decreased from 71.1 J/g to 54.2 J/g (Figure 3, Table 3). Also, the typical temperatures of this effect shift to lower temperatures: T_{onset} from 111°C to 108°C; T_{max} from 143 °C to 140 °C; T_{end} varies from 176°C to 175°C. At the same time, the mass loss of this compound decreases from 3.9 wt % to 3.1 wt % (Table 3).

It was estimated that the heat of exothermic effect at 830–890°C practically did not change till 336 h but by prolonging the hydrothermal treatment duration till 504 h, decreased to 47.8 J/g (Figure 3, Table 4). Also, the typical temperatures of this effect shift to higher temperatures: T_{onset} from 857°C to 858°C; T_{peak} from 868°C to 870°C; T_{end} from 878°C to 882°C. Besides, the mass loss remained the same (Table 4).

At the same time, the total amount of water in the formed calcium silicate hydrate structure slightly decreased by prolonging the synthesis duration from 120 h to 504 h (Figure 4) and can be expressed:

(3.3 wt% H_2O) 168 h < τ < 168 h (4.1 wt% H_2O)

This data is in a good agreement with other scientists results [25, 26].

Table 3

Parameters of endothermic effect at 80–200 °C for varying durations of hydrothermal treatment

Duration of hydrothermal treatment, h	T_{onset}, °C	T_{max}, °C	T_{end}, °C	Mass loss, %	Heat of reaction, J/g
120	111	143	175	3.9	71.1
168	115	145	177	3.6	69.3
336	108	140	174	3.3	55.1
504	108	140	175	3.1	54.2

Table 4

Parameters of exothermic effect at 830–890C at varying durations of hydrothermal synthesis

Duration of hydrothermal treatment, h	T_{onset}, °C	T_{max}, °C	T_{end}, °C	Mass loss, %	Heat of reaction, J/g
120	857	868	878	0.2	49.9
168	855	866	876	0.2	49.9
336	857	869	880	0.2	49.1
504	858	870	882	0.2	47.8

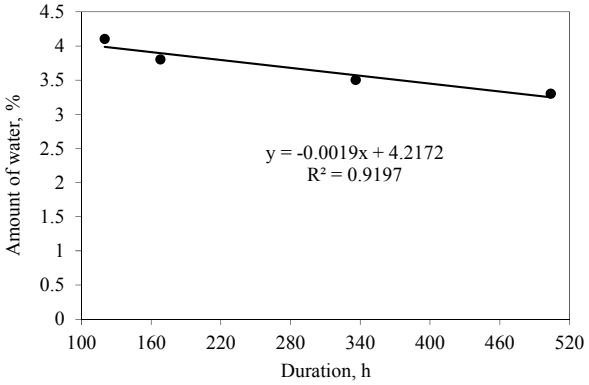

Fig. 4 - Dependence of amount of water in synthesis product structure on the duration of hydrothermal treatment.

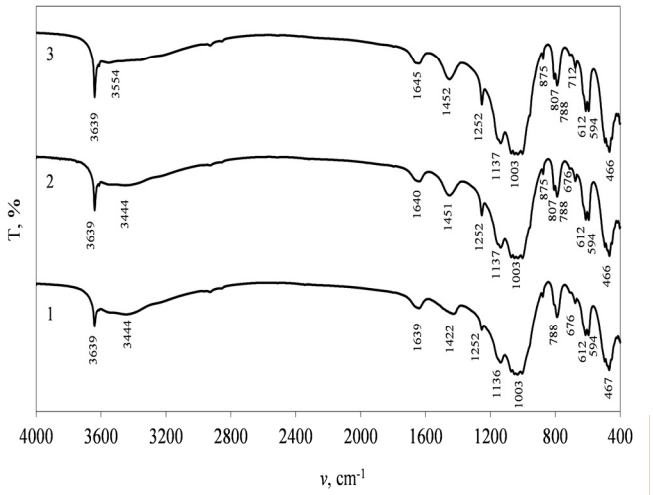

Fig. 5 - IR spectra of synthesis product for varying durations of hydrothermal synthesis at 200 °C, in h: 1 – 168, 2 – 336, 3 –504.

FT-IR analysis data support the above mentioned results. It was found that hydrothermal treatment duration has influence on the width of absorption bands and peak intensities. It was determined that by prolonging treatment duration to 504 h, a sharp peak near 3639 cm^{-1} becomes more sharper and shows the decrease of the intensity of the H_2O bending and stretching bands (Figure 5, curves 2–3). A wide band near 3444 – 3554 cm^{-1} indicates that molecular water forms hydrogen bridges in the interlayers. The decrease of this band intensity shows the lower quantity of molecular H_2O in synthesis product structure (Figure 5, curves 2–3). Also, additional stretching bands at about 1252 and 807 cm^{-1} can be assigned to cross-linked tetrahedral units, formed due to polymerization of the single silicate sheets to double sheets, thus forming a framework (Q^4) (Figure 5, curves 2–3). Garbev et al. has determined that these bands are assigned to truscottite [27].

The experimental data and theoretical hypothesis were also supported by thermodynamic calculations. Recrystallization reactions of gyrolite that are possible during the hydrothermal synthesis at 200°C are given below:

$$2CaO{\cdot}3SiO_2{\cdot}2.5H_2O + 10H_2O \rightarrow$$
$$\rightarrow 1/4(7CaO{\cdot}12SiO_2{\cdot}3H_2O) + 0.25Ca(OH)_2 +$$
$$+ 11.5H_2O, \text{ truscottite} \quad (1)$$

$$2CaO{\cdot}3SiO_2{\cdot}2.5H_2O + 10H_2O \rightarrow$$
$$\rightarrow 1/3(6CaO{\cdot}6SiO_2{\cdot}H_2O) + SiO_2 + 12.17H_2O,$$
Xonotlite (2)

$$2CaO{\cdot}3SiO_2{\cdot}2.5H_2O + 10H_2O \rightarrow$$
$$\rightarrow 0.4(5CaO{\cdot}6SiO_2{\cdot}5.5H_2O) + 0.6SiO_2 + 10.3H_2O,$$
1.1 nm tobermorite (3)

$$2CaO{\cdot}3SiO_2{\cdot}2.5H_2O + 10H_2O \rightarrow$$
$$\rightarrow 1.5(CaO{\cdot}2SiO_2{\cdot}2H_2O) + 0.5Ca(OH)_2 + 9H_2O,$$
okenite (4)

$$2CaO{\cdot}3SiO_2{\cdot}2.5H_2O + 10H_2O \rightarrow$$
$$\rightarrow 0.4(5CaO{\cdot}6SiO_2{\cdot}10.5H_2O) + 0.6SiO_2 + 8.3H_2O,$$
1.4 nm tobermorite (5)

$$2CaO{\cdot}3SiO_2{\cdot}2.5H_2O + 10H_2O \rightarrow$$
$$\rightarrow 1.5(CaO{\cdot}2SiO_2{\cdot}2H_2O) + 0.5Ca(OH)_2 + 9H_2O,$$
Z-phase (6)

The theoretical possibilities of the truscottite (curve 1), xonotlite (curve 2), 1.1 nm tobermorite (curve 3), okenite (curve 4), 1.4 nm tobermorite (curve 5) and Z-phase (curve 6) formation reactions are given in the Figure 6 $\Delta_r G_T^0 = f(T)$ plot and in Table 5.

The thermodynamic parameters of reactions (Figure 6, Table 5) showed, that the negative values of $\Delta_r G_T^0$ would be reached only at higher than 150°C temperature for all studied reactions. Moreover, by increasing the temperature most likely reactions 1 and 2 would occur, meanwhile the thermodynamic possibility of reaction (3) is significantly lower even if calculated $\Delta_r G_T^0$ value are negative. Thus, it can be seen that during the hydrothermal treatment at 200°C temperature the greatest possibility that gyrolite will transform into

Table 5

Thermodynamic data of reaction dependence on temperature for truscottite (1) and Z-phase (6) formation reactions at 373–548K

Reactions	T, K	373	398	423	448	473	498	523	548
1	$\Delta_r H_T^0$, kJ	105.1	108.4	111.7	115.1	118.3	121.6	124.9	128.2
	$\Delta_r S_T^0$, J	256.0	264.5	272.5	280.1	287.2	294.0	300.4	306.6
	$\Delta_r G_T^0$, kJ	9.6	3.1	-3.5	-10.4	-17.5	-24.7	-32.2	-39.8
2	$\Delta_r H_T^0$, kJ	149.9	152.5	154.9	157.4	159.9	162.5	165.0	167.5
	$\Delta_r S_T^0$, J	333.1	339.7	345.8	351.6	357.0	362.2	367.1	371.8
	$\Delta_r G_T^0$, kJ	25.7	17.2	8.7	-0.01	-8.8	-17.8	-26.9	-36.2
6	$\Delta_r H_T^0$, kJ	-32.4	-31.0	-29.6	-28.3	-26.9	-25.5	-24.2	-22.8
	$\Delta_r S_T^0$, J	-187.6	-184.0	-180.7	-177.6	-174.6	-171.8	-169.1	-166.6
	$\Delta_r G_T^0$, kJ	37.5	42.2	46.7	51.2	55.6	59.9	64.2	68.4

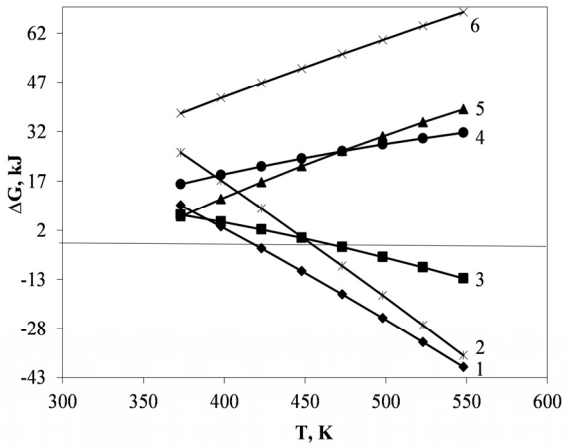

Fig. 6 - Gibbs free energy values as a function of temperature for truscottite (curve 1), xonotlite (curve 2), 1.1 nm tobermorite (curve 3), okenite (curve 4), 1.4 nm tobermorite (curve 5) and Z-phase (curve 6) formation reactions at 373–548 K.

truscottite because the obtained Gibbs free energy value of this compound is the lowest one (ΔG = -39.8 kJ) (Figure 6, curve 1, and Table 5). Reaction (2) could also influence the process; however, its thermodynamic possibility is lower than the first ones (ΔG = -36.2 kJ) (Figure 6, curve 2). It should be noted that the formation of Z-phase in such conditions is the least probable, and it still decreases with increasing temperature (ΔG = -79.1kJ) (Figure 6, curve 6, and Table 5).

It has to be noted that duration of hydrothermal treatment has influence on synthesis products structure as well as its specific surface area (Tab. 6). It was determined that S_{BET} of product was equal to 46.0 m^2/g after 168 h of isothermal treatment. Prolonging the hydrothermal synthesis duration to 336h, the value of S_{BET} decreased to 35.8 m^2/g. Besides, this tendency was observed also after 554 h of treatment.

As it was expected, the pore volume of the synthesis product samples also decreased from 78.8 to 68.8 mm^3/g (Figure 7, a). Besides, the pores with 2.0–5.0 nm radius were dominated in the gyrolite structure after 168 h of synthesis (Figure 7, b). Meanwhile, the pores with 3.0–5.0 nm and even larger radius started to form after 336 h of hydrothermal treatment (Figure 7, c). One of the main reason could be the formation of new compound – truscottite. This tendency of pores growth remains by continuing isothermal treatment (up to 504 h), because the pores with 3.0–6.0 nm and 6.0–10.0 radius is dominated in the synthesis product (Figure 7, d).

In the next stage of experiment there was done Zn^{2+} ions adsorption by using gyrolite (synthesized after 168 h at 200°C) and clinoptilolite samples (Figure 8).

Table 6

Parameters of specific surface area (S_{BET}) of synthesis product

Duration of hydro-thermal treat-ment, h	Sample mass *m*, g	BET equation constants		Capaticy of mono layer X_m, g	S_{BET}, m^2/g	$C_{BET} = \frac{1}{I \cdot X_m}$ Constant C_{BET}	Reliability coefficient R^2
		Slope $S=tg\alpha$	Intercept *I*				
1	**2**	**3**	**4**	**5**	**6**	**7**	**8**
168	0.036	2095.7	7.0	0.0005	46.0	284.2	0.9991
336	0.063	1606.3	16.3	0.0006	35.8	99.5	0.9995
504	0.062	1735.4	15.7	0.0006	33.4	111.2	0.9994

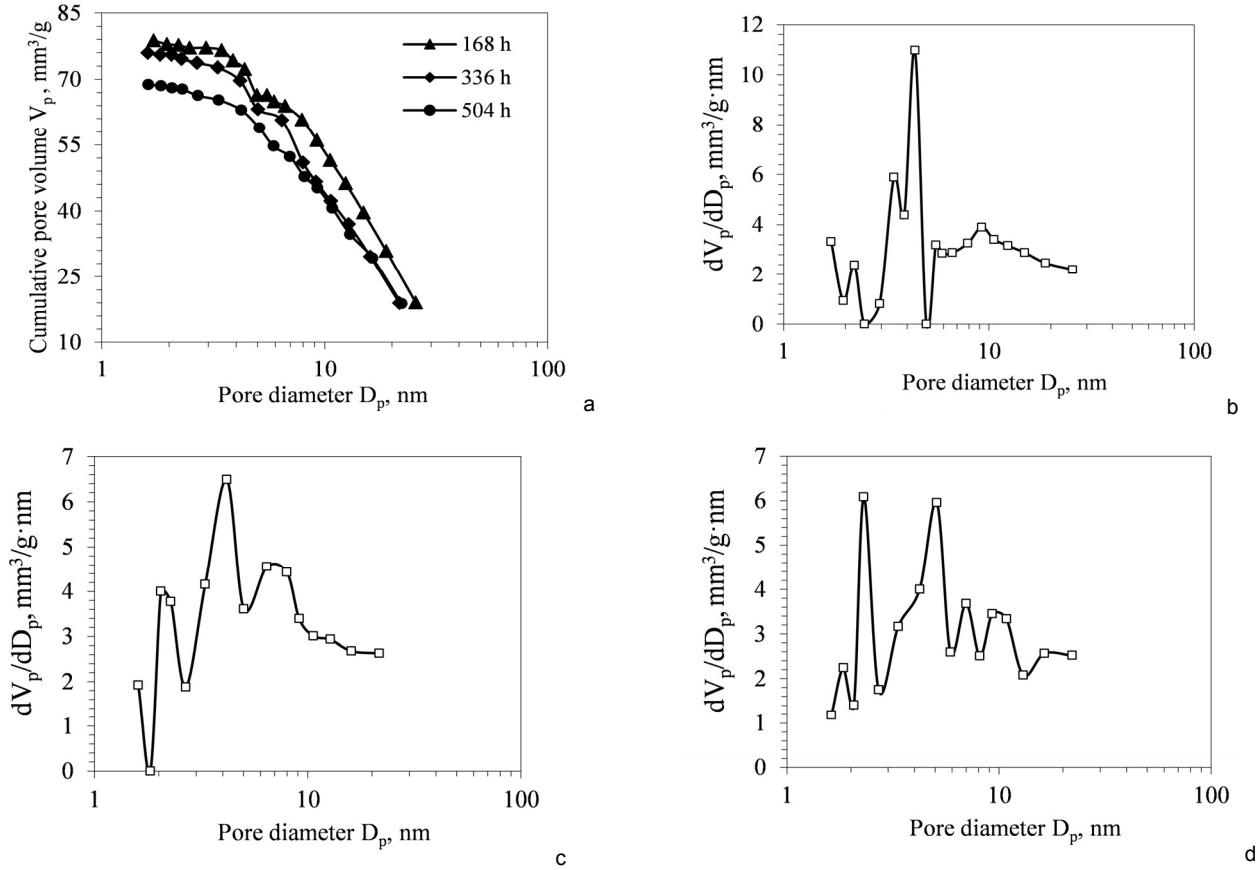

Fig. 7- Total pore volume (a) and differential pore volume plot (b - d) of synthesis product, at varying durations of hydrothermal treatment at 200 °C in, h: b – 168, c – 336, d –504.

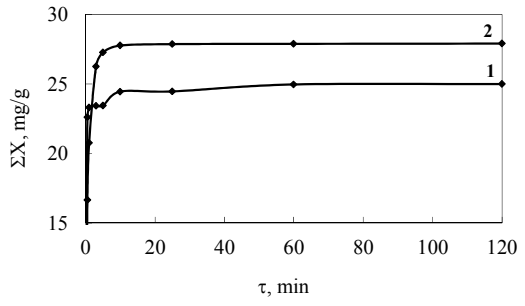

Fig. 8 - Integral kinetic curves of Zn^{2+} ions adsorption from $Zn(NO_3)_2 \cdot 6H_2O$ solution, when Zn^{2+} initial concentration was equal to 0.3 $g \cdot Zn^{2+}/dm^3$; adsorbents: 1 – clinoptilolite; 2 – gyrolite

It was found that the reaction equilibrium is achieved at different periods: after five minutes when gyrolite was used (Figure 8, curve 2), and after 2–3 min – with clinoptilolite (Fig. 8, curve 1). However, at the end of the process, a considerable amount of Zn^{2+} ions (27.91 mg Zn^{2+}/g) was incorporated into the structure of gyrolite, while clinoptilolite adsorbed a smaller quantity (25.00 mg Zn^{2+}/g). After adsorption experiment, gyrolite and clinoptilolite powders were dried and poured into decarbonized water for leaching test. It was determined that the amount of zinc ions leached from gyrolite and clinoptilolite to aqueous medium was below the detection limit (0.0155 mmol/g).

It should be noted, that in order to evaluate multiplew adsorbates, which are commonly found in waste waters, the further research is needed to determine the simultaneous adsorption capacity of gyrolite for heavy metals mixture.

4. Conclusions

1. It was determined that in the CaO – amorphous SiO_2 – H_2O system, when CaO/SiO_2 ratio equals to 0.66, after 120 – 168 h of hydrothermal treatment, gyrolite formed as the final product, because the increment of the intensities (from 112.55 to 130.57 a. u.) and crystallite size (from 46.2 nm to 55.3 nm) of the main diffraction peak (d ~ 2.273 nm) were observed. Also, the mass loss of this compound decreased from 4.1 wt % to 3.3 wt %. Meanwhile, after 336 – 504 h of treatment, gyrolite becames metastable because traces of a new compound of calcium silicate hydrate – truscottite were formed.

2. The calculated thermodynamic parameters of hypothetical recrystallization reactions of gyrolite confirmed the obtained experimental results: the formation of truscottite is more possible because the obtained Gibbs free energy value of this compound is the lowest one (ΔG = -39.8 kJ). Meanwhile, the formation of Z-phase in such conditions is the least probable, and it still decreases with increasing temperature.

3. It was found that S_{BET} value of gyrolite was equal to 46.0 m^2/g after 168 h isothermal curing and by prolonging the hydrothermal synthesis duration till 336 h, S_{BET} of the product decreased to 35.8 m^2/g. Also, the pore volume of the product decreased from 78.8 to 68.8 mm^3/g but the tendency of pores growth remains by continuing isothermal curing (up to 504 h).

4. It was determined that gyrolite has a higher adsorption capacity because the amount of incorporated Zn^{2+} ions into the structure of gyrolite was equaled to 27.91 mg Zn^{2+}/g, meanwhile clinoptilolite adsorbed a smaller quantity (25.00 mg Zn^{2+}/g). Also, it was found that the cation exchange reactions are specific to chemisorption process.

Acknowledgments.
This research was funded by a grant (No. MIP – 025/2014) from the Research Council of Lithuania.

REFERENCES

1. A. Rozycka, L. Kotwica, and J. Malolepszy, Synthesis of single phase gyrolite in the CaO-quartz-Na_2O-H_2O system, Materials Letters, 2014, **120**, 166.
2. V. Kasperaviciute, K. Baltakys, and R. Siauciunas, The sorption properties of gyrolite for cooper ions. Ceramic Silicaty, 2008, **52**(2), 95.
3. A. Bankauskaite, and K. Baltakys, The sorption of cooper ions by gyrolite in alkaline solution. Materials Science – Poland, 2009, **27**(3), 899.
4. S.A. El-Korashy. Cation Exchange of alkali metal hydroxides with some hydrothermally synthesized calcium silicate compounds, Journal of Ion Exchange, 2004, **15**(1), 2.
5. K. Baltakys, A. Eisinas, I. Barauskas, E. Prichockiene, and E. Zaleckas, Removal of Zn(II),Cu(II) and Cd(II) from aqueous solution using gyrolite, Journal of Science and Industrial Research, 2012, **71**, 566.
6. A. Stumm, K. Garbev, G. Beuchle, L. Black, P. Stemmermann, and R. Nuesch, Incorporation of zinc into calcium silicate hydrates, Part I: formation of C–S–H(I) with C/S=2/3 and its isochemical counterpart gyrolite, Cement and Concrete Research, 2005, **35**, 1665.
7. S. Shaw, C. M. B. Henderson, and S. M. Clark, In-situ synchrotron study of the kinetics, thermodynamics, and reaction mechanisms of the hydrothermal crystallization of gyrolite, American Mineralogist, 2002, **87**, 533.
8. A. Bankauskaite, K. Baltakys, A. Eisinas, and S. Zadaviciute, Study on adsorption of heavy metal ions in wastewater by synthetic layered inorganic adsorbents, Desalination and Water Treatment, In Press, available online 26 August 2014; doi: 10.1080/19443994.2014.951074.
9. M.K. Doula, Simultaneous removal of Cu, Mn and Zn from drinking water with the use of clinoptilolite and its Fe-modified form, Water Research, 2009, **43**, 3659.
10. M. A. Winters, J. D. Richter, S. L. Sagar, A. L. Lee, and R. J. Lander, Plasmid DNA purification by selective calcium silicate adsorption of closely related impurities, Biotechnology Progress, 2003, **19**(2), 440.
11. A. Iljina, K. Baltakys, and A. Eisinas, The effect of gyrolite structure properties on Zn^{2+} ion adsorption, Desalination and Water Treatment, In Press, available online 26 August 2014; doi: 10.1080/19443994.2014.978387.
12. A. Baltušnikas, I. Lukošiūtė, and K. Baltakys, XRD Characterization of Organically Modified Gyrolite, Materials Science (Medžiagotyra), 2009, **15**(4), 325.
13. E. P. Flint, H. F. McMurdie, L. S. Wells, Formation of hydrated calcium silicate as elevated temperatures and pressures, Journal of Research of the National Bureau of Standards, 1938, **21**, 617.
14. A. L. Mackay, and H. F. W. Taylor, Gyrolite, Mineralogical Magazine, 1953, **30**, 80.
15. G. L. Kalousek, E. B. Nelson, Hydrothermal reactions of dicalcium silicate and silica, Cement and Concrete Research, 1978, **8**, 283.
16. L. Stevula and J. Petrovic, Formation of an intermediate C-S-H phase during the hydrothermal synthesis of gyrolite, Cement and Concrete Research, 1983, **13**, 684.
17. L. Stevula, M. Harman, I. Horvath, and K. Putyera, The mineral gyrolite and its stability under hydrothermal conditions, Ceramic-Silikaty, 1990, **34**, 315.
18. R. Jauberthie, M. Temimi, and M. Laquerbe, Hydrothermal transformation of tobermorite gel to 10 A° tobermorite, Cement and Concrete Research, 1996, **26**(9), 1335.
19. S. Shaw, C. M. B. Henderson, and S. M. Clark, In-situ synchrotron study of the kinetics, thermodynamics, and reaction mechanism of the hydrothermal crystallization of gyrolite $Ca_{16}Si_{24}O_{60}(OH)_8 \cdot 14H_2O$, American Mineralogist, 2002, **87**, 533.
20. R. A. Chalmers, V. C. Farmer, R. I. Harker, S. Kelly, and H. F. W. Taylor, Mineralogical Magazine, 1964, **33**, 821.
21. R. Siauciunas, and K. Baltakys, Formation of gyrolite during hydrothermal synthesis in the mixtures of CaO and amorphous SiO_2 or quartz, Cement and Concrete Research, 2004, **34**, 2029.

22. Ph. Blanc, X. Bourbon, A. Lassin, and E.C. Gaucher, Chemical model for cement-based materials: Temperature dependence of thermodynamic functions for nanocrystalline and crystalline C–S–H phases, Cement and Concrete Research, 2010, **40**, 851.
23. К.П. Мищенко и А.А. Равделя, Краткий справочник физико-химических величин» под редакцией Л.: Химия, 1974 г– 200 стр.
24. K. Garbev, Ph.D. Thesis, Faculty of Geology and Geography, St. Kliment Ohridski University, Sofia, 2004.
25. J. A. Gard, T. Mitsuda, H. F. W. Taylor, Some observations on Assarsson's Z-phase and its structural relations to gyrolite, truscottite, and reyerite, Mineralogical Magazine, 1975, **40**, 325.
26. E. E. Lachowski, L. W. Murray, H. F. W. Taylor, Truscottite" composition and ionic substitutions, Mineralogical Magazine, 1979, **43**, 333.
27. K. Garbev, B. Gasharova, A. Stumm, L. Black, Y. L. Mathis, and P. Stemmermann, Phase transition of gyrolite into truscottite upon thermal treatment as studied at the ANKA infrared and XRD beamlines, Mineralogische und Technische Kristallographie, 2004, **21**, 118.

****

MANIFESTĂRI ŞTIINȚIFICE / SCIENTIFIC EVENTS

The 6th AMAZON & PACIFIC GREEN MATERIALS CONGRESS will be integrated with the SUSTAINABLE CONSTRUCTION MATERIALS LAT-RILEM CONFERENCE, having in common the motto of "SUSTAINABLE MATERIALS FOR A LIVING WORLD".

APRIL 27- 29th, 2016 ***CALI, COLOMBIA***

Scope and Objectives

Green materials and technology are related to the development and application of materials, products, equipment and systems to the preservation of the environment and natural resources. It looks for the minimization and reduction of the negative impact of human settling and its activities. These concepts are inspired in the criteria of the minimization of the degradation of the environment, Zero or low greenhouse gas emissions (GHG), the conservation of energy and natural resources, and the use of renewable resources.

The event also aims to develop collaborative activities in experimental and theoretical aspects of green science and technology, engineering, interdisciplinary research in areas such as naturally occurring materials, biomaterials, new eco-friendly and safer methods and techniques for developing environmentally friendly novel materials in connection with construction, manufacture materials, rural and urban development, and materials for architectonical heritage. The scope also involves, materials for substituting Portland cement (blended cements, alkali activated materials, geopolymers and others), hybrid materials, nanoscience and nanotechnology; the use of residues from agriculture, mining, industrial and domestic activities in the production of construction materials to reduce the impact of pollution on environment, and much more.

Main Topics

Materials and technology for low cost housing and sheltering, including earth based materials and soil construction
Materials for Architectural Heritage, and composite materials in ancient structures.
Natural / synthetic fiber reinforced composites with polymer or ceramic matrices
Alkali- activated materials and geopolymers
Supplementary cementitious materials and byproducts
Tailored materials for housing and civil infrastructure
Valorization and recycling of industrial, mining, agricultural and urban residues as engineering materials
Wood and wood-based materials, bamboo and guadua as construction materials
Durability of materials
Low carbon technologies applied to building materials
Life cycle of materials
Silvio Delvasto Arjona
Ruby Mejía de Gutiérrez

Contact: Phones: +(57 2) 3302436, Fax: +(57 2) 3392450
Universidad del Valle, Facultad de Ingeniería, Escuela de Ingeniería de Materiales.
Calle 13 No.100-00, Edif. 349, Cali, Colombia, materialscongress@correounivalle.edu.co

****